

1 **Running title:** Spatial models for distance sampling
2 **Number of words:** ~3879
3 **Number of tables:** 0
4 **Number of figures:** 5
5 **Number of references:** 29

6 **Spatial models for distance sampling data:**
7 **recent developments and future directions**

8 **David L. Miller^{1*}, M. Louise Burt²,**
9 **Eric A. Rexstad², Len Thomas².**

- 10 *1. Department of Natural Resources Science, University of Rhode Island,*
11 *Kingston, Rhode Island 02881, USA*
12 *2. Centre for Research into Ecological and Environmental Modelling,*
13 *The Observatory, University of St. Andrews, St. Andrews KY16 9LZ, UK*

14 ***Correspondence author. dave@ninepointeightone.net**

Summary

1. Our understanding of a biological population can be greatly enhanced by modelling their distribution in space and as a function of environmental covariates.
2. Density surface models consist of a spatial model of the abundance of a biological population which has been corrected for uncertain detection via distance sampling methods.
3. We offer a comparison of recent advances in the field and consider the likely directions of future research. In particular we consider spatial modelling techniques that may be advantageous to applied ecologists.
4. The methods discussed are available as R packages developed by the authors.
5. Density surface modelling enables applied ecologists to reliably estimate abundances and create maps of animal/plant distribution.

Keywords: abundance estimation, line transect sampling, point transect sampling, population density, wildlife surveys

34 Introduction

35 When surveying biological populations it is increasingly common to record
36 spatially referenced data, for example: coordinates of observations, habitat
37 type, elevation or (if at sea) bathymetry. Spatial models allow for vast data-
38 bases of spatially-referenced data (e.g. OBIS-SEAMAP, Halpin *et al.*, 2009)
39 to be harnessed, enabling investigation of interactions between environmental
40 covariates and population densities. Mapping the spatial distribution of a
41 population can be extremely useful, especially when communicating results
42 to non-experts. Recent advances in both methodology and software have
43 made spatial modelling readily available to the non-specialist (e.g., Wood,
44 2006; Rue *et al.*, 2009). Here we use the term “spatial model” to include any
45 model that includes spatially referenced covariates, not just smooths of loc-
46 ation. This article is concerned with combining spatial modelling techniques
47 with distance sampling (Buckland *et al.*, 2001, 2004).

Distance sampling takes plot sampling (counting all the individuals or groups of objects within a strip or circle) and extends it to the case where detection is not certain. Observers travel along transect centre lines or stand at points and record the distance from the centre line or point to the object of interest (y). These distances are used to estimate the *detection function*, $g(y)$ (bottom left panel, figure 1), by modelling the decrease in detectability with increasing distance from the line or point (conventional distance sampling, CDS). The detection function may also include animal/observer specific covariates (multiple covariate distance sampling, MCDS; Marques *et al.*, 2007). From the fitted detection function, the probability of detection

can be calculated. The estimated probability that an animal is detected, \hat{p}_i , can then be used to calculate abundance as

$$\hat{N} = \frac{A}{a} \sum_{i=1}^n \frac{1}{\hat{p}_i}, \quad (1)$$

where A is the area of the study region, a is the area covered by the survey (i.e., the sum of the areas of all of the strips/circles) and the summation takes place over the n observed individuals (Buckland *et al.*, 2001, Chapter 3). In general distance sampling is more efficient than plot sampling because all objects observed are recorded and only during analysis are observations discarded due to being too far from the line or point transect (outside of the *truncation distance*, specified when fitting the detection function).

When fitting the detection function in a distance sampling analysis, one assumes that the objects of interest are distributed according to some process (Buckland *et al.*, 2001, Section 2.1). It is usually possible to design surveys such that a homogenous process can be assumed so that (with respect to the line) objects are distributed uniformly. This can be achieved, for example, by ensuring that transect lines run perpendicular to geographical features that would attract (or repel) animals or by post-stratification (Buckland *et al.*, 2001, Section 3.7).

Estimators such as eqn (1) are referred to as *design-based* since they rely on the design of the study to ensure inference is valid. This article focusses on *model-based* inference. Using spatially explicit models one can investigate the response of biological populations to biotic and abiotic covariates that vary over the survey area. Model-based inference also enables the use of

68 data from opportunistic surveys, for example, incidental data arising from
69 “ecotourism” cruises (Williams *et al.*, 2006).

70 Our aims in a DSM analysis are usually two-fold: (i) estimating overall
71 abundance and (ii) investigating the relationship between abundance and en-
72 vironmental covariates. As with any predictions which are outside the range
73 of the data, one should heed the usual warnings regarding extrapolation. For
74 example, in a terrestrial study predictions for unsampled habitats may be
75 unreliable. Frequently, maps of abundance or density are required and any
76 spurious predictions can be visually assessed, as well as by plotting a histo-
77 gram of the predicted values. A sensible definition of the region of interest
78 avoids prediction outside the range of the data.

79 This article focuses on those recent advances in spatial modelling of dis-
80 tance sampling data which are of most utility to applied ecologists. These
81 methods are available in the R packages **Distance** and **dsm**, and will soon
82 be available in the popular Windows application Distance (Thomas *et al.*,
83 2010).

84 Throughout this article a motivating data set is used to illustrate the
85 methods. These data are from a combination of several shipboard surveys
86 conducted on pantropical spotted dolphins (*Stenella attenuata*) in the Gulf
87 of Mexico. 47 groups of dolphins were observed; group size was recorded, as
88 well as the Beaufort sea state at the time of the observation. Coordinates for
89 each observation and bathymetry data were also available as covariates for
90 the analysis. A complete example analysis is provided as an online appendix.

91 The rest of the article follows this structure: we first introduce the dens-
92 ity surface modelling approach of Hedley & Buckland (2004); explain how

93 to estimate abundance and uncertainty; then go on to describe recent ad-
 94 vances and provide practical advice regarding model fitting, formulation and
 95 checking. Before concluding, we look at two alternative (but less mature)
 96 methods which take a more direct approach to modelling spatial distance
 97 sampling data.

98 Density surface modelling

99 This section focuses on modelling the density/abundance estimation stage
 100 of distance sampling, using the “count model” of Hedley & Buckland (2004),
 101 which we refer to as *density surface modelling* (DSM). Both line and point
 102 transects can be used but if lines are used then they are split into con-
 103 tiguous *segments* (indexed by j), which are of length l_j . Segments should
 104 be small enough such that the density does not vary appreciably within a
 105 segment (usually making the segments approximately square, $2w \times 2w$, is
 106 sufficient). Count or estimated abundance is then modelled as a smooth
 107 function of covariates using a generalized additive model (GAM; e.g. Wood,
 108 2006). For each segment or point, the response is modelled as a function of
 109 environmental covariates (the z_{jk} with k indexing the covariates, e.g., loca-
 110 tion, sea surface temperature, weather conditions). The covered area enters
 111 the model as an offset: the area covered at segment j is $A_j = 2wl_j$ and at
 112 point j is $A_j = w\pi^2$ (where w is the truncation distance).

The model for the count per segment is:

$$\mathbb{E}(n_j) = \exp \left[\log_e (\hat{p}_j A_j) + \beta_0 + \sum_k f_k (z_{jk}) \right],$$

114 where the f_k s are smooth functions of the covariates and β_0 is an intercept
 115 term. Multiplying the covered area (A_j) by the probability of detection
 116 (\hat{p}_j) gives the *effective area* for segment j . If there are no covariates other
 117 than distance in the detection function then the probability of detection is
 118 constant (i.e., $\hat{p}_j = \hat{p}$, $\forall j$). The distribution of n_j can then be modelled as
 119 overdispersed Poisson, negative binomial, or Tweedie distribution (see *Recent*
 120 *developments*, below).

121 Figure 1 (top panel) shows the raw observations of the dolphin data, along
 122 with the transect lines, overlaid on the depth data. Figure 2 shows a GAM
 123 fitted to the dolphin data, the top panel shows predictions from a model
 124 where depth was the only covariate, the bottom panel shows predictions
 125 where a (bivariate) smooth of spatial location was also included.

126 Abundance estimation is not the only information that can be derived
 127 from these models. Plots of marginal smooths of the spatially referenced
 128 covariates show the relationships between the covariates and abundance. The
 129 effect of depth on abundance for the dolphin data can be seen in Figure 3.

An alternative to modelling counts would be to use the per-segment/circle
 abundance can be estimated using distance sampling methods and the es-

timated counts used as the response. In this case we replace n_j by:

$$\hat{N}_j = \sum_{r=1}^{R_j} \frac{s_{jr}}{\hat{p}_j},$$

131 where R_j is the number observations in segment j and s_{jr} is the size of the
132 r^{th} group in segment j (if the animals occur individually then $s_{jr} = 1, \forall j, r$).

The following model is then fitted:

$$\mathbb{E}(\hat{N}_j) = \exp \left[\log_e (A_j) + \beta_0 + \sum_k f_k (z_{jk}) \right],$$

133 where \hat{N}_j , as with n_j , is assumed to follow an overdispersed Poisson, negative
134 binomial, or Tweedie distribution. Note that the offset is now the area rather
135 than effective area of the segment/point.

136 *DSM with covariates at the observation level*

137 The above models consider the case where the covariates are measured at
138 the segment/point level. Often covariates (z_{ij} , for individual/group i and
139 segment/point j) are collected on the level of observations; for example sex,
140 group size or observer identity. In this case the probability of detection is a
141 function of the individual level covariates $\hat{p}(z_i)$. Individual level covariates
142 can be incorporated into the model by adopting the following estimator of
143 the per-segment abundance:

$$\hat{N}_j = \sum_{r=1}^{R_j} \frac{s_{jr}}{\hat{p}(z_{ij})}.$$

144 By not including an offset, but instead dividing the count (or estimated

145 abundance) by the area of the segment, we can also model density rather
146 than abundance. We concentrate on abundance here, see Hedley & Buckland
147 (2004) for further details on modelling density.

148 PREDICTION

149 To calculate an abundance estimate for a region of interest, covariates in-
150 cluded in the model must be available at each prediction point at the required
151 resolution (using prediction grid cells that are smaller than the resolution of
152 the spatially referenced data will not have an effect on abundance/density
153 estimates). The areas of the segments/points are included as an offset in the
154 model, so the area of the prediction cells must be included in the prediction
155 data. Predictions are made for the each grid cell using covariate values asso-
156 ciated with each cell and abundance estimates are produced for a particular
157 area by summing predicted values over corresponding grid cells.

158 VARIANCE ESTIMATION

159 Estimating the variance of abundances calculated using a DSM is not straight
160 forward: uncertainty from the estimated parameters of the detection function
161 must be incorporated into the spatial model. A second consideration is that
162 in a line transect survey, adjacent segments are likely to be correlated; failing
163 to account for this spatial autocorrelation will lead to artificially low variance
164 estimates and hence misleadingly narrow confidence intervals.

165 Hedley & Buckland (2004) describe a method of calculating the variance
166 in the abundance estimates using a parametric bootstrap, resampling from
167 the residuals of the fitted model. The bootstrap procedure is as follows.

168 Denote the fitted values for the model to be $\hat{\boldsymbol{\eta}}$. For $b = 1, \dots, B$ (where
169 B is the number of resamples required).

170 1. Resample (with replacement) the per-segment residuals, store the val-
171 ues in \mathbf{r}_b .

172 2. Refit the model but with the response set to $\hat{\boldsymbol{\eta}} + \mathbf{r}_b$ (where $\hat{\boldsymbol{\eta}}$ are the
173 fitted values from the original model).

174 3. Take the predicted values for the new model and store them.

175 From the predicted values stored in the last step the variance originating in
176 the spatial part of the model can be calculated. The total variance of the
177 abundance estimate (over the whole region of interest or sub-areas) can then
178 be found by combining the variance estimate from the bootstrap procedure
179 with the variance of the probability of detection from the detection function
180 model (using the delta method which assumes that the two components of
181 the variance are independent; Seber, 1982).

182 The above procedure assumes that there is no correlation in space between
183 segments however, if many animals are observed in a particular segment then
184 we might expect there to be high numbers in the adjacent segments. A
185 moving block bootstrap (MBB; Efron & Tibshirani, 1993, Section 8.6) can
186 account for some of this spatial autocorrelation in the variance estimation.
187 The segments are grouped together into overlapping blocks, (so if the block
188 size is 5, block one is segments 1, \dots , 5, block two is segments 2, \dots , 6, and so
189 on). Then, at step (2) above, resamples are taken of the blocks (contiguous
190 collections of segments) rather than individual segments within the transects.

191 Using blocks should account for some of the autocorrelation between the
192 segments, inflating the variances accordingly. However, because the block size
193 dictates the maximum amount of spatial autocorrelation accounted for, this
194 may not fully account for the autocorrelation. These bootstrap procedures
195 can also be modified to take into account detection function uncertainty by
196 generating new distances from the fitted detection function and then re-
197 calculating the offset by fitting a detection function to the new distances.

198 Recent developments

199 *GAM uncertainty and variance propagation*

200 Rather than using a bootstrap, one can use GAM theory to construct uncer-
201 tainty estimates for DSM abundance estimates. This merely requires that
202 we use the distribution of the parameters in the model to simulate model
203 coefficients, using them to generate possible abundance estimated (further
204 information can found in Wood, 2006, page 245). Such an approach removes
205 the need to refit the model many times, making variance estimation much
206 faster.

207 Williams *et al.* (2011) go a step further and incorporate the uncertainty
208 in the estimation of the detection function into the variance of the spatial
209 model, albeit only when only environmental covariates are in the DSM. Their
210 procedure is as follows:

- 211 1. Fit a density surface model.
- 212 2. Re-fit the model with an additional term that characterises the uncer-

213 tainty in the estimation of the detection function (via the derivatives
214 of the probability of detection, \hat{p}).

215 3. Variance estimates of the abundance calculated using standard GAM
216 theory will include uncertainty from the estimation of the detection
217 function.

218 We consider that propagating the uncertainty in this manner is not only more
219 computationally efficient but also preferable from a technical perspective. A
220 moving block bootstrap does not fully account for spatial autocorrelation;
221 assuming that the residuals are exchangeable when they are not will lead to
222 wider confidence intervals. In simulation the confidence intervals produced
223 via the above method are narrower than their bootstrap equivalents, while
224 maintaining good coverage.

225 DSM uncertainty can be visualised via a plot of per-cell coefficient of
226 variation obtained by dividing the standard error for each cell by its predicted
227 abundance. Figure 4 shows a map of the coefficient of variation for the
228 model which includes both location and depth covariates using the variance
229 propagation method.

230 EDGE EFFECTS

231 Recent work (Ramsay, 2002; Wang & Ranalli, 2007; Wood *et al.*, 2008; Scott-
232 Hayward *et al.*, Submitted; Miller & Wood, Submitted) has highlighted the
233 need to take care when smoothing over areas with complicated boundaries;
234 e.g., those with rivers, peninsulae or islands. If two parts of the domain
235 (either side of a river or inlet, say) are inappropriately linked by the model

236 (the distance between the points is measured as a straight line, rather taking
 237 into account obstacles) then the boundary feature can be “smoothed across”
 238 leading to incorrect inference. Ensuring that a realistic spatial model has
 239 been fitted to the data is essential for valid inference. The soap film smoother
 240 of Wood *et al.* (2008) is particularly appealing as the model jointly estimates
 241 boundary conditions for a complex study area along with the interior smooth.
 242 This can be particularly helpful when uncertainty is estimated via a bootstrap
 243 as the model helps avoid large, unrealistic predictions which can plague other
 244 smoothers (Bravington & Hedley, 2009).

245 Even if the study area does not have a complicated boundary, edge effects
 246 can still be problematic. Miller *et al.* (In prep) show that global smoothers
 247 which have unpenalized plane components tend to cause the fitted surface to
 248 increase unrealistically as predictions move further away from the locations
 249 of survey effort. They suggest the use of Duchon splines (a generalisation of
 250 thin plate regression splines) to alleviate the problem.

251 TWEEDIE DISTRIBUTION

252 The Tweedie distribution offers a very flexible alternative to the quasi-Poisson
 253 and negative binomial distributions as a response distribution when model-
 254 ling count data (Candy, 2004). Through the parameter λ , many common
 255 distributions arise; varying λ between 1 (Poisson) and 2 (gamma) leads to
 256 a random variable which is a sum of M gamma variables where M is Pois-
 257 son distributed (Jørgensen, 1987). The distribution does not change appre-
 258 ciably when λ is changed by less than 0.1 therefore, a simple line search
 259 over the possible values of λ is usually reasonable. Mark Bravington (pers.

comm.) suggested plotting the square root of the absolute value of the residuals against fitted values; a “flat” plot (points forming a horizontal line) give an indication of a “good” value for λ . We additionally suggest using the metrics described in the next section for model selection.

Practical advice

Figure 5 shows a flow diagram of the modelling process for creating a density surface model for distance sampling data. The diagram shows which methods are compatible with each other and what the options are for modelling a particular data set.

In our experience, it is sensible obtain a detection function which fits the data as well as possible and only after a satisfactory detection function has been obtained, begin spatial modelling. Model selection can be performed for the detection function using AIC and model checking using goodness-of-fit tests given in Buckland *et al.* (2004). If animals occur in groups rather than individually, bias can be incurred due to the higher visibility of larger groups. Bias due to group size can be assessed by regressing evaluations of the fitted detection function onto the logarithm of group size, then comparing the expected and observed values of the group size at zero distance, if there is a large difference then it may be necessary to include size as a covariate in the detection function see (see Buckland *et al.*, 2001, Section 4.8.2.4). The bottom right panel of figure 1 shows a such a plot with the regression line overlaid.

For the spatial model, smooth terms can also be selected using (approx-

imate) p -values. A useful technique for covariate selection is to have an additional penalty to each term in the GAM which allows smooth terms to be removed from the model during fitting (Wood, 2006, Section 4.1.6). Generalized cross validation (GCV) score (or related metrics such as UnBiased Risk Estimator or REstricted Maximum Likelihood score; UBRE and REML, respectively) and percentage deviance explained are useful for model selection. We highly recommend the use of standard GAM diagnostic plots. Wood (2006), Chapter 5, provides practical information on GAM model selection and fitting.

In the analysis of the dolphin data, we included a smooth of location. This not only nearly doubles the percentage deviance explained (27.3% to 52.7%), it also allows us to account for spatial autocorrelation (in a primitive way). One can see this when comparing the two plots in Figure 2 and the plot of the depth in Figure 1, the plot of the smooth of depth alone looks very similar to the raw plot of the depth data. A smooth of an environmental-level covariate such as depth can be very useful for assessing the relationships between abundance and the covariate (as in Figure 2). Caution should be employed when interpreting smooth relationships and abundance estimates, especially if there are gaps over the range of covariate values; large counts may occur at a high value of depth but if no further observations occur at such a high value, then investigators should be skeptical of any relationship. For this reason, a smooth of space is recommended for inclusion in candidate models. Limiting the “wigglyness” of smooths of spatial location (by limiting their basis size) can be a useful way of restricting their influence whilst still allowing them to “mop up” the residual spatial correlation in the data.

308 In the analysis presented we have converted from latitude and longitude
309 to kilometres from the centre of the survey region (27.01, -88.3) because the
310 bivariate smoother used (the thin plate spline; Wood, 2003) is isotropic, i.e.
311 it treats the wigglyness of the smoother in each direction as equal. Moving 1
312 degree in latitude is not the same as moving 1 degree in longitude and so using
313 kilometres from the centre of the study region makes the covariates isotropic
314 (using SI units throughout would also remove the need for conversion).

315 Direct modelling of the spatial point process

316 [[LEN: Does some chat about Andy Royle's stuff fit in here?]]

317 Rather than use a GAM to model the spatially explicit part of the model,
318 two recent articles (Johnson *et al.*, 2010; Niemi & Fernández, 2010) have
319 modelled the process using point processes (Cox & Isham, 1980). In both
320 cases the density of objects described by an intensity function, which can
321 include spatially-referenced covariates.

322 Johnson *et al.* (2010) proposes a point process-based model for distance
323 sampling data. They first assume that the locations of all individuals in the
324 survey area (not just those observed) form a realisation of a Poisson process.
325 Parameters of the intensity function are then estimated via standard max-
326 imum likelihood methods for point processes (Baddeley & Turner, 2000). In
327 contrast to Hedley & Buckland (2004), all parameters are estimated jointly
328 so uncertainty from both the spatial pattern and the detection function is
329 incorporated into variance estimates for the abundance. This also ensures
330 that correlations between the detection function and underlying point process

331 are estimated correctly (and do not falsely inflate or deflate variance estim-
332 ates). The authors also addressed the issue of overdispersion unmodelled by
333 spatial covariates (i.e. counts that do not follow a Poisson mean-variance
334 relationship) using a post-hoc correction factor.

335 Niemi & Fernández (2010) also use Poisson processes but incorporate
336 them into a fully Bayesian approach. Model fitting proceeds in two stages:
337 first the detection function is fitted, then the spatial model (via MCMC)
338 assuming the detection function parameters are known, so detection function
339 uncertainty is not incorporated in the spatial model.

340 Both of the above Poisson process models do not account for group size,
341 but both state that this could be included by considering a marked point
342 process (Cox & Isham, 1980, Section 5.5). Both methods offer direct mod-
343 elling of the point process, although with some drawbacks compared to the
344 methodology of Hedley & Buckland (2004). It should be noted that the loss
345 of efficiency from using DSM is not large (Buckland *et al.*, 2004, p. 313)
346 because distances contain little information about spatial variation due to
347 how thin transects are compared to their lengths and how small circles are
348 compared to the study area.

349 Discussion

350 The use of model-based inference for determining abundance and spatial
351 distribution from distance sampling data presents new opportunities in the
352 field of population assessment. Inference from a sample of sightings to a
353 population in a study area does not depend upon a random sample design,

354 and therefore data from "platforms of opportunity" (Williams *et al.*, 2006)
355 can be used.

356 Unbiased estimates are dependent upon either (i) distribution of sampling
357 effort being random throughout the study area (for design-based inference)
358 or (ii) model correctness (for model-based inference). It is easier to have
359 more confidence in the former than in the latter because our models are
360 always wrong. Nevertheless model-based inference will play an increasing
361 role in population assessment as the availability of spatially-references data
362 increases.

363 The field is quickly evolving to allow modelling of more complex data
364 building on the basic ideas of density surface modelling. We expect to see
365 large advances in two areas: temporal inferences and the handling of spa-
366 tial correlation. These should become more mainstream as modern spatio-
367 temporal modelling techniques are adopted. Petersen *et al.* (2011) provided
368 a very basic framework for temporal modelling; their model included smooth
369 terms both before and after the construction of an offshore windfarm. Spa-
370 tial autocorrelation can be accounted for via approaches that explicitly intro-
371 duce correlations such as generalized estimating equations (GEEs; Hardin &
372 Hilbe, 2003) or via mechanisms such as that of Skaug (2006), which allowed
373 observations to cluster according to one of several states (e.g. "feeding" or
374 "transit") taking into account short-term agglomerations ("hot spots"). These
375 advances should assist both modellers and wildlife managers to make optimal
376 conservation decisions. [[LEN: don't like this last sentence but feel like there
377 should be some summing up here]]

378 Acknowledgments

379 DLM wishes to thank Mark Bravington and Sharon Hedley for their help
380 and patience in explaining and providing code for their variance propagation
381 method. **[[LEN: N45 thanks?]]**

382 References

- 383 Baddeley, A. & Turner, R. (2000) Practical maximum pseudolikelihood for spatial
384 point patterns. *Australian & New Zealand Journal of Statistics*, **42**, 283–322.
- 385 Bravington, M. & Hedley, S.L. (2009) Antarctic minke whale abundance estimates
386 from the second and third circumpolar IDCR/SOWER surveys using the
387 SPLINTR model. SC-61-IA14, International Whaling Commission.
388 URL [http://www.iwcoffice.org/_documents/sci_com/sc61docs/](http://www.iwcoffice.org/_documents/sci_com/sc61docs/SC-61-IA14.pdf)
389 SC-61-IA14.pdf
- 390 Buckland, S.T., Anderson, D., Burnham, K.P., Laake, J.L., Borchers, D.L. &
391 Thomas, L. (2001) *Introduction to Distance Sampling*. Oxford University Press.
- 392 Buckland, S.T., Anderson, D., Burnham, K.P., Laake, J.L., Borchers, D.L. &
393 Thomas, L. (2004) *Advanced Distance Sampling*. Oxford University Press.
- 394 Candy, S. (2004) Modelling catch and effort data using generalised linear models,
395 the Tweedie distribution, random vessel effects and random stratum-by-year
396 effects. *Ccamlr Science*, **11**, 59–80.
- 397 Cox, D.R. & Isham, V. (1980) *Point Processes*. Monographs on Applied Probability
398 and Statistics. Chapman and Hall. ISBN 9780412219108.
- 399 Efron, B. & Tibshirani, R.J. (1993) *An Introduction to the Bootstrap*. Chapman &
400 Hall/CRC. ISBN 9780412042317.
- 401 Halpin, P., Read, A., Fujioka, E., Best, B., Donnelly, B., Hazen, L., Kot, C.,
402 Urian, K., LaBrecque, E., Dimatteo, A., Cleary, J., Good, C., Crowder, L. &
403 Hyrenbach, K.D. (2009) OBIS-SEAMAP: The World Data Center for Marine
404 Mammal, Sea Bird, and Sea Turtle Distributions. *Oceanography*, **22**, 104–115.
- 405 Hardin, J. & Hilbe, J. (2003) *Generalized Estimating Equations*. Chapman and
406 Hall/CRC, London, UK.
- 407 Hedley, S.L. & Buckland, S.T. (2004) Spatial models for line transect sampling.
408 *Journal of Agricultural, Biological, and Environmental Statistics*, **9**, 181–199.
- 409 Johnson, D.S., Laake, J.L. & Ver Hoef, J.M. (2010) A model-based approach for
410 making ecological inference from distance sampling data. *Biometrics*, **66**, 310–
411 318.
- 412 Jørgensen, B. (1987) Exponential dispersion models. *Journal of the Royal Statist-*
413 *ical Society. Series B, Statistical Methodology*, **49**, 127–162.
- 414 Marques, T.A., Thomas, L., Fancy, S. & Buckland, S.T. (2007) Improving estimates
415 of bird density using multiple-covariate distance sampling. *The Auk*, **124**, 1229–
416 1243.

- 417 Miller, D.L., Jones, E. & Matthiopoulos, J. (In prep) Reliable spatial smoothing
418 without edge effects.
- 419 Miller, D.L. & Wood, S.N. (Submitted) Finite area smoothing with generalized
420 distance splines. pp. 1–27.
- 421 Niemi, A. & Fernández, C. (2010) Bayesian Spatial Point Process Modeling of Line
422 Transect Data. *Journal of Agricultural, Biological, and Environmental Statistics*,
423 **15**, 327–345.
- 424 Petersen, I.K., MacKenzie, M.L., Rexstad, E.A., Wisz, M.S. & Fox, A.D. (2011)
425 Comparing pre- and post-construction distributions of long-tailed ducks *Clan-*
426 *gula hyemalis* in and around the Nysted offshore wind farm, Denmark: a quasi-
427 designed experiment accounting for imperfect detection, local surface features
428 and autocorrelation. 2011-1, Centre for Research into Environmental and Eco-
429 logical Modelling, University of St Andrews.
430 URL <http://research-repository.st-andrews.ac.uk/handle/10023/2008>
- 431 Ramsay, T. (2002) Spline smoothing over difficult regions. *Journal of the Royal*
432 *Statistical Society. Series B, Statistical Methodology*, **64**, 307–319.
- 433 Rue, H., Martino, S. & Chopin, N. (2009) Approximate Bayesian inference for
434 latent Gaussian models by using integrated nested Laplace approximations. *J.*
435 *R. Statist. Soc. B*, **71**, 319–392.
- 436 Scott-Hayward, L.A.S., MacKenzie, M.L., Donovan, C.R., Walker, C.G. & Ashe,
437 E. (Submitted) Complex Region Spatial Smoother (CReSS).
438 URL <http://research-repository.st-andrews.ac.uk/handle/10023/2048>
- 439 Seber, G.A.F. (1982) *The Estimation of Animal Abundance and Related Paramet-*
440 *ers*. Blackburn Pr. ISBN 9781930665552.
- 441 Skaug, H.J. (2006) Markov modulated Poisson processes for clustered line transect
442 data. *Environmental and Ecological Statistics*, **13**, 199–211.
- 443 Thomas, L., Buckland, S.T., Rexstad, E.A., Laake, J.L., Strindberg, S., Hedley,
444 S.L., Bishop, J.R., Marques, T.A. & Burnham, K.P. (2010) Distance software:
445 design and analysis of distance sampling surveys for estimating population size.
446 *Journal of Applied Ecology*, **47**, 5–14.
- 447 Wang, H. & Ranalli, M. (2007) Low-rank smoothing splines on complicated do-
448 mains. *Biometrics*, **63**, 209–217.
- 449 Williams, R., Hedley, S.L., Branch, T.A., Bravington, M.V., Zerbini, A.N. & Find-
450 lay, K.P. (2011) Chilean blue whales as a case study to illustrate methods to
451 estimate abundance and evaluate conservation status of rare species. *Conserva-*
452 *tion Biology*, **25**, 526–535.

- 453 Williams, R., Hedley, S.L. & Hammond, P. (2006) Modeling distribution and
454 abundance of Antarctic baleen whales using ships of opportunity. *Ecology and*
455 *Society*, **11**, 1.
- 456 Wood, S.N. (2003) Thin plate regression splines. *Journal of the Royal Statistical*
457 *Society. Series B, Statistical Methodology*, **65**, 95–114.
- 458 Wood, S.N. (2006) *Generalized Additive Models: An introduction with R*. Chapman
459 & Hall/CRC.
- 460 Wood, S.N., Bravington, M.V. & Hedley, S.L. (2008) Soap film smoothing. *Journal*
461 *of the Royal Statistical Society. Series B, Statistical Methodology*, **70**, 931–955.

462 Figures

Fig. 1 Top: the survey area, transect centrelines and observations with size of circle corresponding to the group size overlaid onto depth data; bottom left, histogram of observed distances with fitted detection function; bottom right, plot of evaluations of the fitted detection function at given distances versus the logarithm of group size with linear trend showing the relation between probability of detection (given distance) and group size.

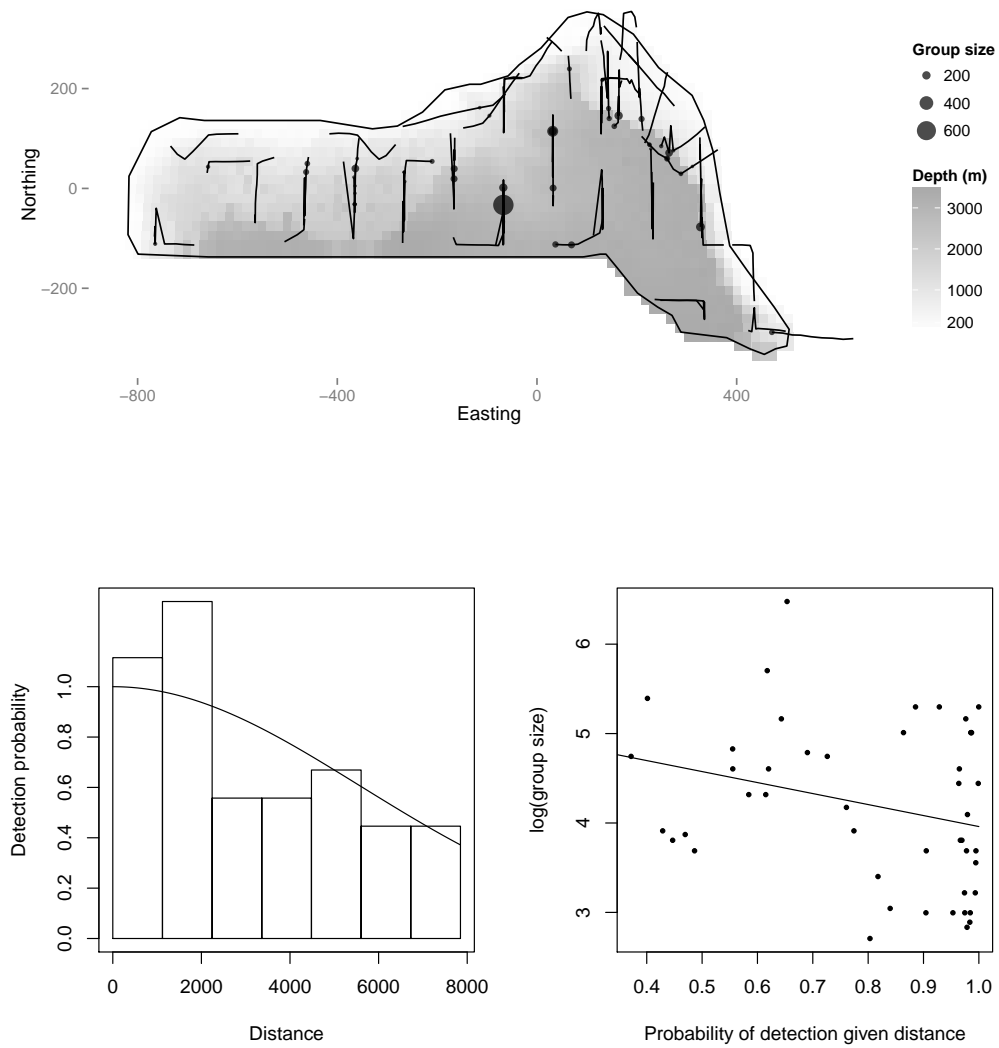


Fig. 2 Predictions for the dolphin data. Top: Predictions from the model using only depth as an explanatory variable, bottom: the model using both depth and location.

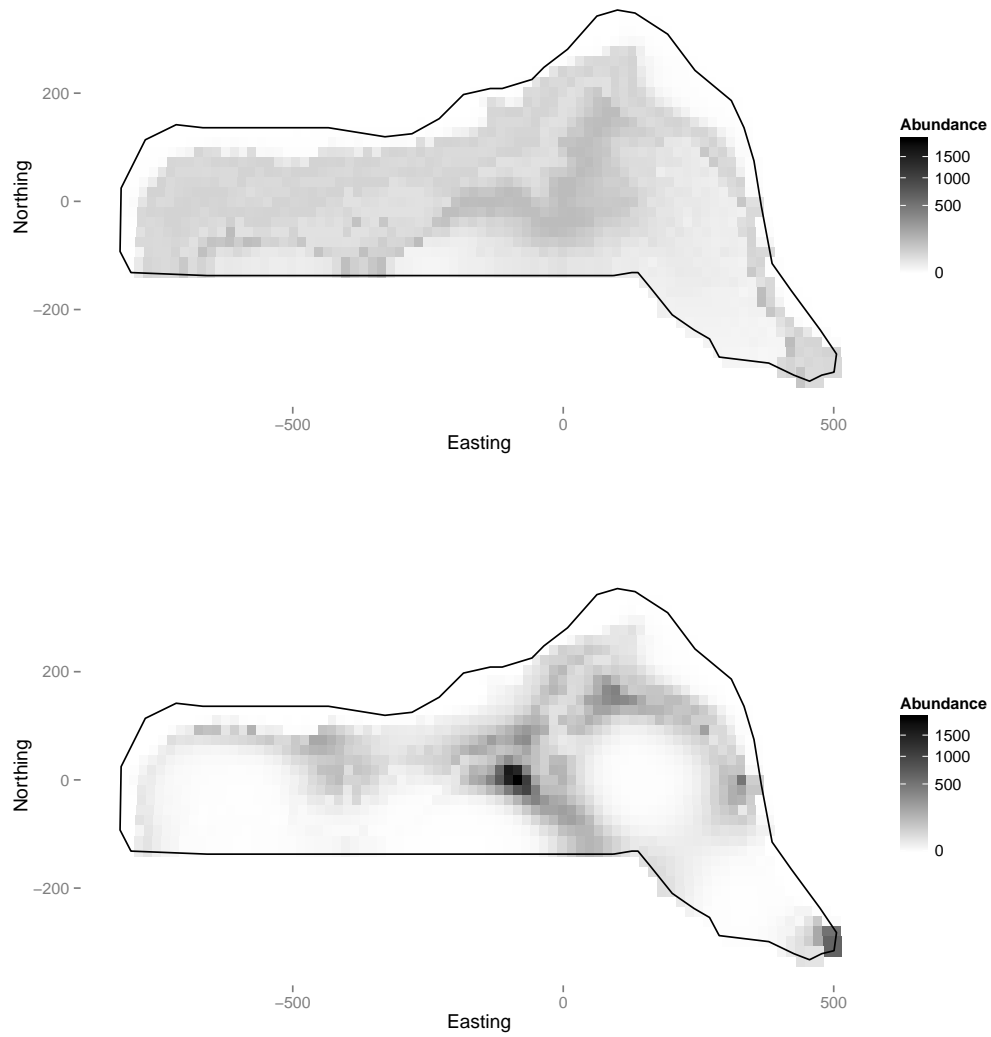


Fig. 3 Plot of the effect on the response of depth (from the model with both depth and location smooths), note that it is possible to draw a straight line between 750m and 3000m within the confidence band (between the dashed lines), so the wiggles in the smooth may not be indicative of any relationship. What is clear is that there is some effect up to about 500m. The rug ticks at the bottom of the plot indicate we have good coverage of the range of depth values in the survey area. Note that the y axis in such plots is on the scale of the link function (log in this case), so care should be taken in their interpretation.

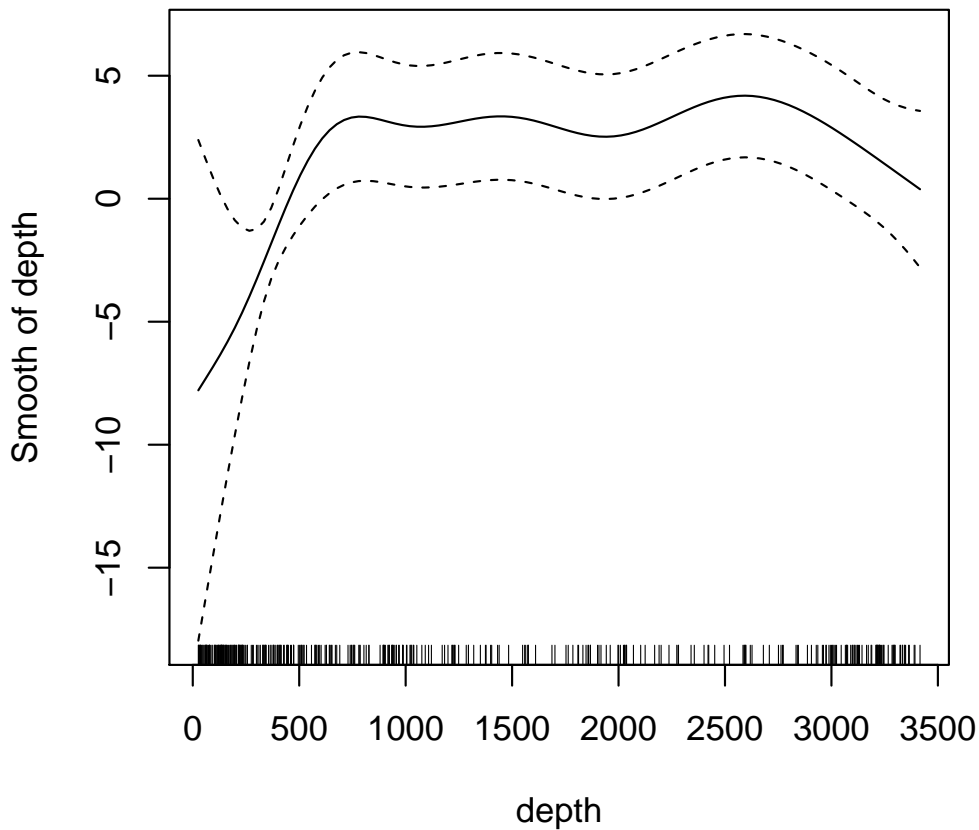


Fig. 4 Plot of coefficient of variation map for the model with smooths of both depth and location. Uncertainty was estimated using the variance propagation method of Williams *et al.* (2011). As might be expected, there is high uncertainty where there is low sampling effort (comparing to figure 1).

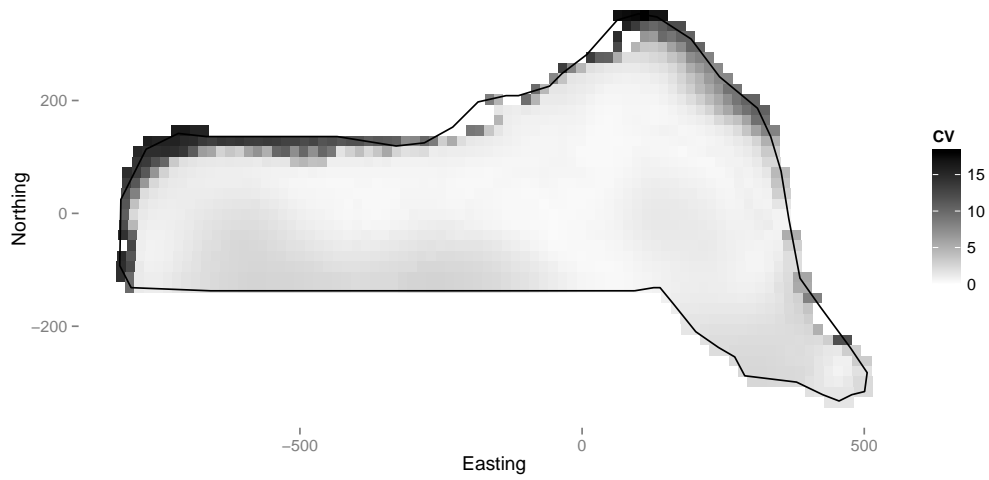


Fig. 5 Flow diagram showing the modelling process for creating a density surface model.

